

## Article

# Fault Detection and Diagnosis for Plasticizing Process of Single-Base Gun Propellant Using Mutual Information Weighted MPCA under Limited Batch Samples Modelling

Mingyi Yang<sup>1,2,3,4,\*</sup>, Junyi Wang<sup>1,2,4</sup>, Yinlong Zhang<sup>4</sup>, Xinlin Bai<sup>1,2,4</sup>, Zhigang Xu<sup>1,2,3,4,\*</sup>, Xiaofang Xia<sup>5</sup> and Linlin Fan<sup>3,4</sup>

- <sup>1</sup> State Key Laboratory of Robotics, Shenyang Institute of Automation, Chinese Academy of Sciences, Shenyang 110016, China; jywang@sia.cn (J.W.); baixinlin@sia.cn (X.B.)  
<sup>2</sup> Institutes for Robotics and Intelligent Manufacturing, Chinese Academy of Sciences, Shenyang 110169, China  
<sup>3</sup> University of Chinese Academy of Sciences, Beijing 100049, China; fanlinlin@sia.cn  
<sup>4</sup> Shenyang Institute of Automation, Chinese Academy of Sciences, Shenyang 110016, China; zhangyinlong@sia.cn  
<sup>5</sup> School of Computer Science and Technology, Xidian University, Xi'an 710071, China; xiaofangxia89@gmail.com  
\* Correspondence: myyang@sia.cn (M.Y.); zgxu@sia.cn (Z.X.)

**Abstract:** Aiming at the lack of reliable gradual fault detection and abnormal condition alarm and evaluation ability in the plasticizing process of single-base gun propellant, a fault detection and diagnosis method based on normalized mutual information weighted multiway principal component analysis (NMI-WMPCA) under limited batch samples modelling was proposed. In this method, the differences of coupling correlation among multi-dimensional process variables and the coupling characteristics of linear and nonlinear relationships in the process are considered. NMI-WMPCA utilizes the generalization ability of a multi-model to establish an accurate fault detection model in limited batch samples, and adopts fault diagnosis methods based on a multi-model *SPE* statistic contribution plot to identify the fault source. The experimental results demonstrate that the proposed method is effective, which can realize the rapid detection and diagnosis of multiple faults in the plasticizing process.

**Keywords:** gun propellant; plasticizing process; fault detection and diagnosis; principal component analysis; normalized mutual information; Bayesian inference; early warning of failure



**Citation:** Yang, M.; Wang, J.; Zhang, Y.; Bai, X.; Xu, Z.; Xia, X.; Fan, L. Fault Detection and Diagnosis for Plasticizing Process of Single-Base Gun Propellant Using Mutual Information Weighted MPCA under Limited Batch Samples Modelling. *Machines* **2021**, *9*, 166. <https://doi.org/10.3390/machines9080166>

Academic Editor: Dongsheng Yang

Received: 1 July 2021

Accepted: 8 August 2021

Published: 12 August 2021

**Publisher's Note:** MDPI stays neutral with regard to jurisdictional claims in published maps and institutional affiliations.



**Copyright:** © 2021 by the authors. Licensee MDPI, Basel, Switzerland. This article is an open access article distributed under the terms and conditions of the Creative Commons Attribution (CC BY) license (<https://creativecommons.org/licenses/by/4.0/>).

## 1. Introduction

With the improvement in the level of automation in the modern process industry, the process scale is becoming larger and more complicated, and people are paying more and more attention to the safety and consistency of product quality [1–4]. In the process of explosive production, stricter requirements in the safety, reliability, and product quality of the system are being put forward because of its special working environment. As the energy source of a variety of bullets and small guns [5,6], single-based gun propellant plays a pivotal role in the field of explosives. At present, the research in the field of single-based gun propellant mainly focuses on the performance test of new formulations and new processes [7,8], component detection [9], invalidation prediction [10], and so on, but rarely involves the fault detection and monitoring and warning of abnormal conditions in the production process. The plasticizing process is an important process in the single-based gun propellant production process, which plays a crucial role in the molding and product quality of single-based gun propellant [11]. However, at present, the plasticizing process can only achieve simple fault alarm of process variables by means of alarm threshold or rate of change exceeding the limit, and lacks the ability of gradual fault detection with the small amplitude and the ability of abnormal alarm and evaluation of the operating condition.

So, there is a huge potential safety hazard in the production process of single-based gun propellant, which affects the product quality and restricts the increase of production. Therefore, in the monitored field of the propellant production process, it has become an urgent demand to establish a reasonable and effective online monitoring and fault detection mechanism to quickly and to accurately monitor and identify and then eliminate all kinds of abnormal working conditions in the process of propellant production process.

In recent years, because of the wide application of distributed control systems (DCSs) and the development of machine learning technology, data-driven process monitoring methods have been applied in fault detection in some industries [12–17]. Among them, the multivariate statistical process monitoring method represented by principal component analysis (PCA) has attracted extensive attention [18], because it only requires process data under normal working conditions to establish a monitoring model, which is especially suitable for industrial processes with few fault samples [19], and provides a new idea for plasticizing process monitoring of single-based gun propellant. However, the traditional PCA method can only be applied to a continuous process, while the single-based gun propellant plasticization has the property of batch process, and its data set has one more batch dimension than that of the continuous process [20], so we cannot use PCA and other methods directly. Multiway principal component analysis (MPCA) can process batch process data. At present, MPCA has been widely used in process monitoring of the batch process. In the meantime, some improved methods based on MPCA have been proposed in recent years. An adaptive MPCA method was proposed for condition monitoring and fault diagnosis by Zhang [21], which used a weighted recursive algorithm to update the covariance matrix adaptively, and adjusted the effect of the new data on the final model parameters by weighting them. Peres [22] proposed the Pareto Variable Selection (PVS) MPCA method to monitor batch processes described by high-dimensional datasets. Zhou [23] proposed a sub-period division strategies combined with MPCA to diagnose the faults in the sequence batch reactor of a wastewater treatment process. However, the MPCA method and its various improvement strategies [24] are still linear modelling methods, and the application of them in batch process monitoring will inevitably lead to higher false and missed alarms. Therefore, many scholars have proposed a variety of nonlinear methods [25–29].

However, these methods above always use a single linear or nonlinear analysis method, whereas the actual operation trajectory of plasticizing process is complicated coupling in three axes, namely: time, batch. and variable. The coupling relationship between the multidimensional variable is often a variety of linear and nonlinear correlations coexisting at the same time, and it is difficult to achieve a data comprehensive analysis of the potential characteristics using the analysis of a single method. At the same time, the characteristics and mechanism of the plasticizing process are complex, showing strong batch variation characteristics and slow time-varying drift characteristics, so that abnormal changes will be easily covered by the deviation from normal state, and the coupling relationship between the multi-dimensional process variables is also different. If all of the characteristics well are not balanced, the potential information extracted from the model cannot describe the running state of the process comprehensively and effectively. Therefore, to ensure the rapidity and reliability of fault monitoring in the plasticizing process of single-based gun propellant, the monitoring method must be able to deal with the above two problems simultaneously.

For the first problem, because mutual information cannot only reflect the linear correlation between variables, but also represents their nonlinear correlation, many scholars have integrated it with statistical process monitoring methods based on multivariate methods to carry out process monitoring, and have achieved positive results [30–35]. Among them, the mutual information principal component analysis (MI-PCA) method proposed by Tong [30] and the MI-KPCA proposed by Huang [33] are more representative. Secondly, for the problem of correlation differences among variables, Ge [36], Tong [37], and Jiang [38] divided the variables into multi-block from the perspective of the statistical

characteristics of data, and then proposed a process monitoring method based on the distributed PCA (DPCA). To some extent, the DPCA method can distinguish the correlation between variables, so it can achieve better result of fault detection than the traditional PCA method. However, all of the above methods require sufficient and large amounts of modelling data. For batch processes, in general, to meet the basic requirements of statistical analysis, the number of batches should be at least two to three times that of the process variable [39]. When there are only limited batch modelling data, only a few operation batches at each sampling time cannot provide accurate and reliable statistical information in the direction of the batch. However, the production process of single-based gun propellant has high risk coefficient and there are many manual interventions. Different starting conditions, batch cycles, and various products make it present different process characteristics. While ensuring the accuracy and reliability of fault detection, it will have more practical significance for the plasticization process if we can use the limited batch data to realize few-shot learning and rapid modelling.

Transfer learning can realize few-shot learning, but it needs the data and knowledge of the source domain to solve the learning of target domain [40,41]. In this paper, a fault detection and diagnosis method based on normalized mutual information weighted multiway principal component analysis (NMI-WMPCA) under limited batch sample modelling (the number of batches of modelling data is equivalent to the dimension of process variables) was proposed. The method does not require any source domain data and knowledge, and takes into account the differences of coupling correlation among multi-dimensional process variables and the mixed characteristics of multi-linear and non-linear relations contained in the process simultaneously. Firstly, the intricate coupling relationship between multidimensional variables is characterized by normalized mutual information, and the correlation between variables of different dimensions is modified by weight. Then, the data sets that reflect the coupling relationship between each variable and the other dimension variables are obtained, and the corresponding monitoring models are established. Finally, according to the Bayesian inference, the monitoring results of different models are fused into a set of global monitoring statistics to realize the process monitoring. NMI-WMPCA utilizes the generalization ability of the multi-model to establish an accurate fault detection model in limited batch samples, and adopts the fault diagnosis method based on a multi-model square prediction error (*SPE*) statistics contribution plot to identify the fault sources. The experimental results demonstrate that the proposed method is effective. The rapid detection of multiple faults and the early warning of abnormal conditions in the plasticization process can be realized by using only limited batch sample modelling, and the fault can be diagnosed and analyzed.

## 2. Basic Theories and Methods

### 2.1. The Plasticizing Process of Single-Base Gun Propellant and Its Batch Process Attribute

Single-base gun propellant is essentially plasticized gunpowder containing nitrocellulose (NC), which is usually prepared by a solvent extrusion molding process. The main raw materials are mixed cotton composed of two kinds of NC with different nitrogen contents and a small amount of stabilizer (diphenylamine (DPA)). The process flow chart of the single-base gun plasticization process is shown in Figure 1. It uses ether-ethanol mixed solvent to dissolve NC, and a kneaded plasticizing machine is utilized to transform the nitrocellulose-containing chemicals into plastic materials with uniform mixing and a compact structure for the subsequent molding process. The plasticizing machine makes the materials subject to mutual friction, squeezing, tearing, and stretching through the relative rotation of a pair of agitating blades, so as to complete the kneading and plasticizing of the materials. The basic operation flow of the process can be described as feeding, plasticizing process, waiting for discharging, finishing discharging, cleaning, and waiting for feeding. The process parameters of the plasticizing process mainly include component content and ratio, plasticizing temperature, plasticizing time, stirring force, stirring speed, etc. At

present, the quality effect of the plasticized materials still needs on-site evaluation by a process technician, making its process safety even more important.

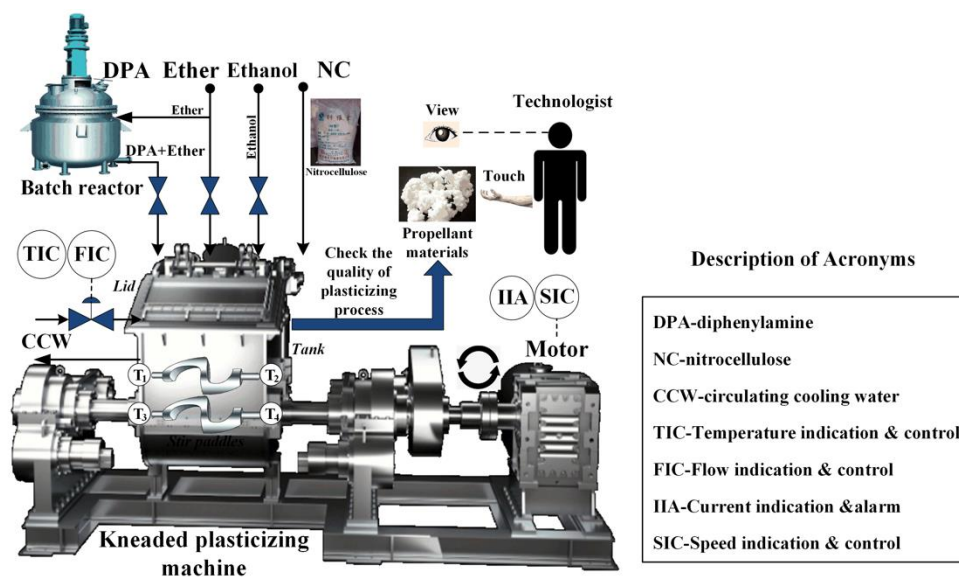


Figure 1. The process flow diagram of the plasticizing process.

The plasticization process studied in this paper uses a kneaded plasticizing machine to complete the plasticization of the single-base gun propellant material. It is an intermittent production process with obvious batch process attributes and characteristics. The discontinuous operation of materials and the complex coupling relation of temperature and energy in the batch process [42] result in strong nonlinear and dynamic time-varying characteristics. Its statistical characteristics (such as mean and variance) will change over time, and each batch shows strong batch changes, and each batch exhibits slow drift characteristics, resulting in the status monitoring and monitoring of the batch process. Fault diagnosis is more complicated and challenging than continuous processes [19]. In the plasticizing process, each tank of the propellant material is defined as a batch. Assuming that the process has  $J$  process variables, and  $K$  data points can be collected for each variable in a single batch, then a batch can form a two-dimensional matrix  $X_i(J \times K)$ . The batch operation is repeated  $B$  times, and  $B$  two-dimensional matrices  $X_i(J \times K)(i = 1, 2 \dots B)$  can be obtained. So, a three-dimensional data matrix  $\bar{X}(B \times J \times K)$  can be used to represent the data set of the single-base gun plasticization process, where  $B$  is the number of batches,  $J$  is the number of variables, and  $K$  is the number of sampling points.

## 2.2. Process Monitoring Method Based on Multiway Principal Component Analysis (MPCA)

Principal component analysis (PCA) is a linear dimensionality reduction method based on multivariate projection [43]. Its main idea is to convert high-dimensional space into low-dimensional space, and to retain high-dimensional information as much as possible. Assuming that there are  $m$  sensors collecting in the process, and each sensor sampling  $n$  times, the data matrix is formed as  $X = [x(1), x(2) \dots x(n)]^T \in \mathbb{R}^{n \times m}$ , and the PCA model decomposes  $X$  into:

$$X = \hat{X} + E = TP^T + E \quad (1)$$

$$T = XP \quad (2)$$

$$\hat{X} = TP^T = \sum_{j=1}^A t_j p_j^T \quad (3)$$

$$E = X - \hat{X} = X(I - PP^T) \quad (4)$$

among them, the main component reconstruction matrix is  $\hat{X}$ ; the residual matrix is  $E \in R^{n \times m}$ ;  $P = [p_1, p_2 \dots p_A] \in R^{m \times A}$  and  $T = [t_1, t_2 \dots t_A] \in R^{n \times A}$  are the main component load matrix and the score matrix, respectively; and  $A$  represents the number of principal components retained in the principal component model.

PCA can usually only be applied to the two-dimensional data matrix  $X(n \times m)$ . For the three-dimensional data matrix  $\bar{X}(B \times J \times K)$  of the plasticization process, multiway principal component analysis (MPCA) unfolds it into a two-dimensional matrix, and then applies the PCA method for statistical analysis to calculate the corresponding score vector and load vector. After that, the appropriate number of principal component  $A$  is reserved to establish an online monitoring model. At present, the commonly used data unfolding methods are batch-wise unfolding and variable-wise unfolding. Batch-wise unfolding gives a two-dimensional data matrix  $\bar{X}(B \times KJ)$ . It retains the batch dimension and merges the data from both the time and variable dimensions. The row vector contains all the variables and time data in each batch production cycle. However, the data matrix obtained by variable-wise unfolding is  $\bar{X}(KB \times J)$ . It keeps the dimension of the process variables unchanged, but merges the data of the batch operation and sampling time. Its column vector contains the values of each variable at all sampling times of all batches. Please refer to the literature [44] for the detailed process.

MPCA only needs the measured values of the variables under normal operating conditions as the modelling data, which reflects the cross-correlation between the process variables and the autocorrelation relationship of the variables themselves. When abnormalities occur in the process, it will lead to changes in the trajectory of the process variables or the coupling relationship between the variables. At the moment, the fault can be detected by monitoring whether the multivariate statistics *Hotelling-T<sup>2</sup>* [45] and the *SPE* control chart [46] of the MPCA model are over the limits. The number of principal components  $A$  is determined by the cumulative variance contribution rate or cross-validation method. The  $T^2$  statistic is defined as follows:

$$T^2 = [t_1, t_2 \dots t_A] \Lambda^{-1} [t_1, t_2 \dots t_A]^T \tag{5}$$

$$\Lambda^{-1} = \frac{1}{n-1} T^T T \tag{6}$$

The control limit of the  $T^2$  statistic, monitoring whether a process failure occurs, obeys the  $F$  distribution [47]:

$$T^2_{A,n,\alpha} \sim \frac{A(n^2-1)}{n(n-A)} F_{A,n-A,\alpha} \tag{7}$$

The *SPE* statistics are defined as follows:

$$SPE = \sum_{i=1}^n t_i^2 - \sum_{i=1}^A t_i^2 = \sum_{i=A+1}^n t_i^2 \tag{8}$$

The control limit of the *SPE* statistics is determined by the estimation method of the weight coefficient  $g$  and the degree of freedom  $h$ :

$$SPE_{k,\alpha} \sim g_k \chi^2_{h,\alpha} \tag{9}$$

$$g_k = v_k / 2m_k, h_k = 2m_k^2 / v_k \tag{10}$$

where  $v_k$  and  $m_k$  are the mean and variance of the squared prediction error at the  $k$ th moment in the modelling data set, respectively.

### 2.3. Mutual Information and Mutual Information Principal Component Analysis (MI-PCA)

In probability theory and information theory, mutual information is the amount of information that measures the statistical correlation between two random variables. It

measures the information shared between variables and can simultaneously evaluate the degree of linear and non-linear correlation between two variables [48].

For two discrete variables  $X$  and  $Y$ , the mutual information  $I(X; Y)$  is defined as:

$$I(X; Y) = \sum_{i=1}^M \sum_{j=1}^N p(x, y) \log \frac{p(x, y)}{p(x)p(y)} \quad (11)$$

where  $p(x, y)$  is the joint distribution of two random variables  $X$  and  $Y$ , and  $p(x)$  and  $p(y)$  are marginal probabilities, respectively. If  $X$  and  $Y$  are independent of each other, this means that when there is no overlapping information, the mutual information value is equal to 0. Conversely, if the correlation between the two is higher, the mutual information value is greater. It can be seen from Equation (11) that the solution of mutual information requires the probability density distribution of the variables  $X$  and  $Y$  to be known. As there is no prior knowledge of the data distribution, the kernel density estimation method is usually used to fit its probability density and to determine the probability value corresponding to the variable [49].

The MI-PCA method uses the mutual information between variables in various dimensions to define the correlation matrix of the data, instead of the covariance matrix in the traditional principal component analysis, so that it can describe the mixed characteristics of linear correlation and nonlinear correlation, and can establish a more accurate monitoring model for the process data.

### 3. Normalized Mutual Information Weighted Multiway Principal Component Analysis (NMI-WMPCA) Method

In order to better deal with the mixed characteristics of various linear and nonlinear relationships contained in the process, and to reflect the differences of the coupling correlation between different dimensional variables, a fault detection and diagnosis method based on normalized mutual information weighted multiway principal component analysis was proposed. It mainly includes three parts: the two-stage unfolding of batch process data, the characterization and weighted correction modelling of multi-dimensional variable coupling relationship, and the fusion of multi-model monitoring information. The advantage of this algorithm is that the complex coupling relationship among the multi-dimensional variables in the process can be described by the normalized mutual information, and according to the correlation degree among the different dimensional variables, different weights are given to each dimensional variable to complete the weighted correction, which fully reflects the correlation difference between the variables in modelling. The mutual information can not only reflect the linear correlation, but also represent the nonlinear correlation among the multi-dimensional variables, so that the corresponding MPCA model can comprehensively mine the various mixed relations and coupling correlation characteristics of the original data, avoiding the loss of useful information.

#### 3.1. Two-Stage Batch Data Unfolding Method of the Plasticizing Process

Ideally, the data of each batch in the plasticizing process should have the same running time. However, the actual plasticizing process of single-based gun propellant is affected by different aspects such as raw material fluctuation, difficult evaluation of plasticizing effect, and interference, which results in the time length of the data of each batch in the plasticizing process being different, and sometimes the difference is great. It is difficult to deal with the problem of uneven-length batches along the direction of batch-wise unfolding, and the future time value needs to be estimated and filled when online applicate, which can easily lead in errors and reduce the monitoring performance. When unfolded along the direction of variable-wise, the correlation between variables at different moments is ignored, and the nonlinearity in the time axis of the process variables cannot be eliminated. As a result, it is not sensitive to the fault, leading to the poor rapidity and sensitivity of fault detection.

Therefore, this paper combines the advantages of batch-wise and variable-wise unfolding, and a two-stage batch data unfolding method was proposed to process the three-dimensional data set in the plasticizing process, as shown in Figure 2. Firstly, the method unfolds the three-dimensional data  $\bar{X}(B \times J \times K)$  of the plasticizing process into a two-dimensional array. Then, the matrix  $X(B \times JK)$  is obtained by standardized processing with mean value of 0 and standard deviation of 1, which can eliminate the nonlinearity and dynamics between the process variables to a certain extent. Finally, the data are rearranged as  $X_{train}(BK \times J)$  along the variable direction, so that it can deal with the uneven-length problem of the batch data. The multiway data two-stage unfolding method not only saves the information between batches, but also does not need to estimate the future value of new batches when it is used for online monitoring. Therefore, the false alarm rate can be reduced, and the reliability and prediction accuracy can be improved.

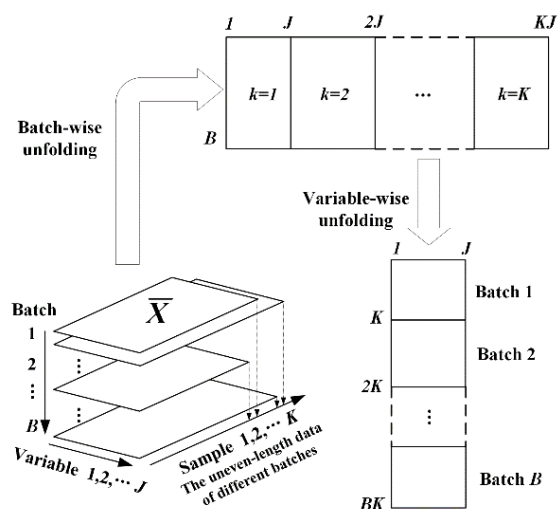


Figure 2. Diagram of the two-stage batch data unfolding for the plasticizing process.

### 3.2. Weighted Correction Modelling Based on Normalized Mutual Information

Weighted correction modelling describes the complex coupling relationship between multi-dimensional process variables by normalized mutual information firstly, and then according to the relationship between the weighted corrected correlation characteristics between the different dimensional variables, which results in a data set that can reflect the coupling relationship between each variable and the other dimensional variables. Then, the condition monitoring MPCA model is built according to the data sets. See Section 4.1 for the specific modelling method and steps, as well as a discussion of the specific calculation method of normalized mutual information value.

In order to facilitate the weighted correction operation, the mutual information needs to be normalized. At present, the commonly used calculation formula is:

$$NMI(X;Y) = \frac{I(X;Y)}{(H(X) + H(Y))/2} \tag{12}$$

where  $NMI$  refers to normalized mutual information.  $H(X)$  and  $H(Y)$  are the information entropy of  $X$  and  $Y$ , respectively, and can indicate the uncertainty degree of the variable value. The initial uncertain degree of  $X$  can be expressed by entropy  $H(X)$ :

$$H(X) = -\sum_{i=1}^M p(x_i) \log p(x_i) \tag{13}$$

The joint entropy between  $X$  and  $Y$  is defined as:

$$H(X, Y) = -\sum_{i=1}^M \sum_{j=1}^N p(x_i, y_j) \log p(x_i, y_j) \quad (14)$$

Joint entropy measures the total uncertain degree of  $X$  and  $Y$ , and its value range is:

$$\max\{H(X), H(Y)\} \leq H(X, Y) \leq H(X) + H(Y) \quad (15)$$

The relationship between mutual information, entropy, and joint entropy is:

$$I(X; Y) = H(X) + H(Y) - H(X, Y) \quad (16)$$

From the two formulas above, it can be seen that the upper bound of mutual information of two random variables is the minimum entropy of the two random variables, and the value range of  $I(X; Y)$  is:

$$0 \leq I(X; Y) \leq \min\{H(X), H(Y)\} \quad (17)$$

Obviously,  $\min\{H(X), H(Y)\} \leq (H(x) + H(y))/2$ . So, it is unreasonable to adopt the normalization form of Equation (12).

Entropy is defined by Jensen's inequality [50]:

$$H(X) \leq \log \sum_{i=1}^M p(x_i) \frac{1}{p(x_i)} = \log M \quad (18)$$

So, we can get  $0 \leq I(X; Y) \leq \min\{\log M, \log N\}$ , where  $M$  and  $N$  represent the possible number of discrete random variables  $X$  and  $Y$ , respectively.

Based on the above analysis,  $NMI$  is defined as the quotient of the mutual information  $I(X; Y)$  and the minimum logarithm of  $M$  and  $N$ .

$$NMI(X; Y) = \frac{I(X; Y)}{\min\{\log M, \log N\}} \quad (19)$$

### 3.3. Multi-Model Information Fusion Strategy Based on Bayesian Inference

$NMI$ - $WMPCA$  established  $J$  different  $MPCA$  models. When applied online, new samples will be monitored by  $J$  different  $MPCA$  models simultaneously, and different statistical information of the  $J$  groups will be obtained. The over-limit of any group of statistics means that the process may enter an abnormal working state, which will lead to over-sensitivity of the monitoring model and increase the probability of false alarm of the system. For this reason, this paper adopts a Bayesian inference strategy [38,51] to integrate the information of all  $MPCA$  models, and to fuse the statistical indicators of multiple  $MPCA$  models into a group of probabilistic indicators.

Taking  $T_i^2$  statistical information as an example, it is assumed that the control limit under confidence coefficient  $\alpha$  is  $C_{T_i^2}$ . Its calculation method is shown in Equation (7), and the probability of sample  $x_i$  ( $i = 1, 2 \dots J$ ) fault is

$$P_{T_i^2}(F|x_i) = \frac{P_{T_i^2}(x_i|F)P_{T_i^2}(F)}{P_{T_i^2}(x_i)} \quad (20)$$

$$P_{T_i^2}(x_i) = P_{T_i^2}(x_i|N)P_{T_i^2}(N) + P_{T_i^2}(x_i|F)P_{T_i^2}(F) \quad (21)$$

In the above formula,  $N$  and  $F$  represent the normal and fault, respectively, and  $P_{T_i^2}(N)$  and  $P_{T_i^2}(F)$  represent the prior probabilities of the normal and fault, respectively, where the confidence coefficient  $P_{T_i^2}(N)$  is  $\alpha$ , and  $P_{T_i^2}(F)$  equals to  $1 - \alpha$ .  $P_{T_i^2}(x_i|N)$  and  $P_{T_i^2}(x_i|F)$

represents the posterior probabilities of the normal and fault, respectively, which can be calculated according to the form of empirical distribution. The calculation method is:

$$P_{T_i^2}(x_i|N) = \exp\left(-\frac{T_i^2}{C_{T_i^2}}\right) \tag{22}$$

$$P_{T_i^2}(x_i|F) = \exp\left(-\frac{C_{T_i^2}}{T_i^2}\right) \tag{23}$$

In this paper, the confidence coefficient limit  $\alpha$  is 99%. Finally, the global statistic index  $BIS_{T_2}$  is obtained according to the weighted fusion form.

$$BIS_{T_2} = \frac{\sum_{i=1}^J P_{T_i^2}(x_i|F)P_{T_i^2}(F|x_i)}{\sum_i P_{T_i^2}(x_i|F)} \tag{24}$$

In the same way, through Bayesian inference, we can get  $BIS_{SPE}$  from the statistic value of  $SPE$ . When  $BIS_{T_2} > 1 - \alpha$  or  $BIS_{SPE} > 1 - \alpha$ , the process is identified as an abnormal state. Otherwise, the process is in a normal working state.

#### 4. Fault Detection and Diagnosis Method Based on NMI-WMPCA

NMI-WMPCA weighted and corrected the batch data of the plasticization process in  $J$  different ways to reflect the correlation difference between the different variable dimensions and other dimensions, and established  $J$  MPCA models accordingly. At the same time, the new batch of data needs to be subjected to the same weighted correction strategy when online monitoring, and then each MPCA model is used to calculate the corresponding statistics. The NMI-WMPCA algorithm flow is shown in Figure 3, which specifically includes three parts: offline modelling, online monitoring, and fault diagnosis.

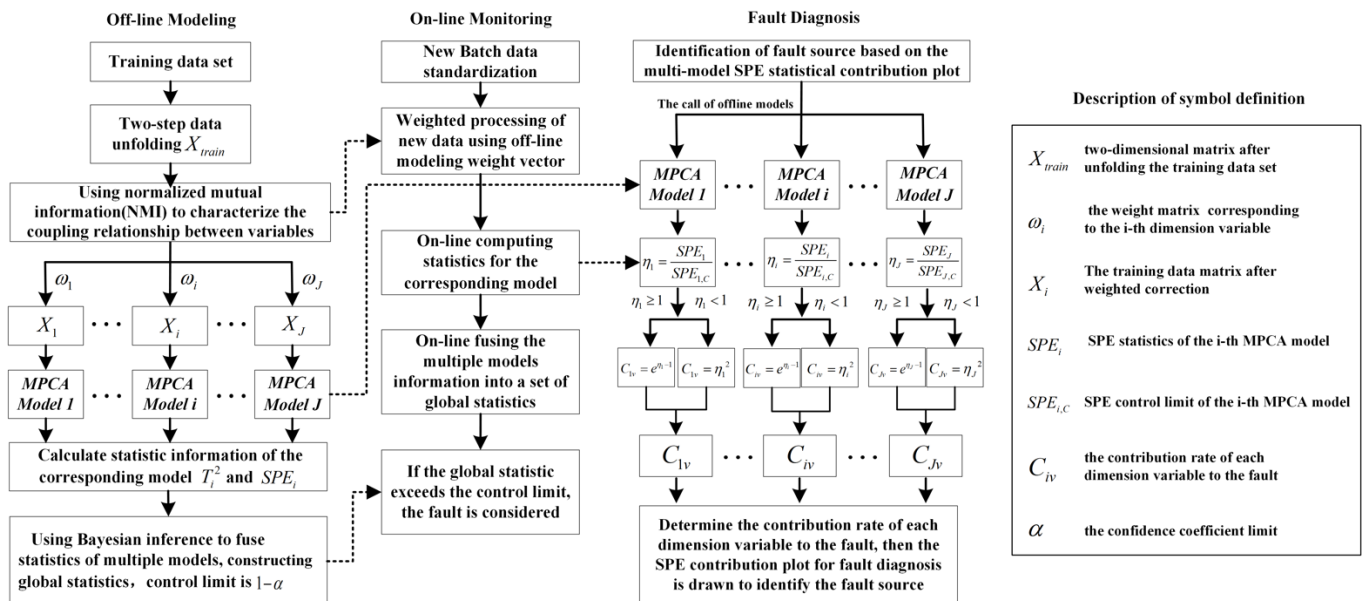


Figure 3. Flowchart of the fault detection and diagnosis based on the NMI-WMPCA method.

##### 4.1. Establish the NMI-WMPCA Model under Normal Working Conditions (Offline Modelling)

- (1) Three-dimensional data unfolding: collect batch data of the plasticization process under normal working conditions as a training data set, and unfold the three-

- dimensional data set according to the method proposed in this article to obtain  $X_{train}(BK \times J)$ ;
- (2) Description of coupling relationship: set the initial value of  $i$  to 1, for the  $i$ -th ( $i = 1, 2 \dots J$ ) dimension process variable  $x_i$ , calculate the normalized mutual information value  $NMI(x_i; x_k)$  between it and each dimension variable  $x_k$  ( $k = 1, 2 \dots J$ ) in  $X_{train}$ ;
  - (3) Weighted correction: determine the weight matrix  $\omega_i$  corresponding to the  $i$ -th dimension variable according to the calculated normalized mutual information value. The formula is:  $\omega_i = diag[NMI(x_i; x_1), NMI(x_i; x_2) \dots NMI(x_i; x_J)]$ , and the unfolded data matrix  $X_{train}(BK \times J)$  is weighted to obtain the training data matrix  $x_i = x_{train} \times \omega_i$ , which reflects the characteristics of the correlation difference between this dimension variable and other dimensions;
  - (4) Model establishment: establish a condition monitoring model based on the MPCA algorithm for  $X_i$ , namely  $X_i = T_i P_i^T + E_i$ , and calculate the  $T_i^2$  and  $SPE_i$  statistics and their control limits;
  - (5) Set  $i = i + 1$ , repeat steps (2) to (4) to obtain  $J$  weighted data sets  $\{X_1, X_2 \dots X_J\}$ , and establish the corresponding  $J$  MPCA state monitoring models;
  - (6) Determine the global statistics  $BIS_{T^2}$  and  $BIS_{SPE}$  constructed by Bayesian inference based on the confidence level  $\alpha$ , and the control limit is  $1 - \alpha$ .

#### 4.2. Online Fault Monitoring of NMI-WMPCA Model

- (1) Online monitoring of the new batch process data  $x_{new}$ , using the mean and standard deviation of the modelling data to standardize the new data;
- (2) Use the weight vector  $\omega_i$  ( $i = 1, 2 \dots J$ ) obtained during modelling to perform weighted fusion processing for the new batch data, namely  $x_{new,i} = x_{new} \times \omega_i$ , to obtain the corresponding  $x_{new,1}, x_{new,2} \dots x_{new,J}$ ;
- (3) Call the model information of each MPCA separately, and calculate the  $T_i^2$  and  $SPE_i$  statistics of  $x_{new,i}$  ( $i = 1, 2 \dots J$ ) under the corresponding MPCA model online;
- (4) Construct new global statistics  $BIS_{T^2}$  and  $BIS_{SPE}$  through Bayesian inference, and fuse the statistics information of the  $J$  groups MPCA models into a set of probabilistic indicators. If the control limit is exceeded, the fault occurs in the process.

#### 4.3. Fault Diagnosis Strategy Based on NMI-WMPCA Model

When a fault is detected, it is necessary to diagnose the fault variable and isolate the variable that caused the fault. The contribution plot method is the most commonly used fault diagnosis method in PCA-based monitoring methods [37]. As the method in this paper contains the monitoring results of  $J$  groups MPCA models, the traditional contribution plot method cannot be used directly. In offline modelling, the normalized mutual information has been used to accurately describe and modify the coupling relationship between each variable and other dimensional variables in the process, and the corresponding MPCA monitoring model has been established. Therefore, the monitoring result of the  $i$ -th MPCA model should be the most directly related to the  $i$ -th dimension variable and can characterize its operating status. According to this internal mechanism, for the NMI-WMPCA monitoring method in this paper, a fault diagnosis method based on the multi-model  $SPE$  statistical contribution plot is proposed to identify the source of the fault. The  $SPE$  statistics and control limits of each MPCA model are used to determine the contribution rate  $C_{iv}$  of each dimension variable to the fault. The specific calculation method is as follows:

$$C_{iv} = \begin{cases} e^{\eta_i - 1}, \eta_i \geq 1 \\ \eta_i^2, \eta_i < 1 \end{cases} \quad (i = 1, 2, \dots, J) \quad (25)$$

where  $\eta_i = SPE_i / SPE_{i,c}$ , and  $SPE_i$  and  $SPE_{i,c}$  are the  $SPE$  statistics and control limits of the  $i$ -th MPCA model, respectively. Obviously, when the  $SPE$  statistic of the  $i$ -th model does not exceed the limit, the contribution rate of the dimensional variable to the fault will

be reduced by the square function. When the *SPE* of the *i*th model exceeds its control limit, the contribution rate of the *i*-th dimensional variable to the fault will be amplified by the exponential function according to its over-limit amplitude so as to realize the identification of the fault source.

## 5. Experiments and Analysis

In this paper, the real plasticizing process data of a certain type single-based gun propellant from Luzhou North Chemical Industries Co., Ltd. were used for the experimental study. Through DCS of the single-based gun propellant production process developed by our team, the batch data of various fault types are generated combined with manual intervention. The correctness and validity of the method proposed in this paper are fully tested and verified.

In this section, the operating conditions of the plasticizing process modelling data are shown in Table 1. The process variables used for modelling are shown in Table 2. In total, 10 process variables of the plasticizing process were selected for monitoring. Each batch of plasticizing time was set to 60 min. However, in order to ensure the plasticizing effect in the production, it was necessary to open the lid of the machine and take samples before the process time was reached, so as to evaluate the plasticizing effect by the on-site technologists, and to give the setting value of the continuous plasticizing time. As a result, the plasticizing time varied from batch to batch. In this paper, 10 batches of data of different lengths were used as the training data sets (the number of batches of modelling data is equivalent to the dimension of process variables) to establish the monitoring models of MPCA, MI-MPCA, and NMI-WMPCA. Then, two normal batches and five faulty batches were used as the test data sets. The sampling interval of a single batch was 10 s, and the data length of each batch used for the modelling ranged from 60 min to 1 h and 28 min. MI-MPCA is an application of MI-PCA in the batch process that was mentioned in literature [30].

**Table 1.** Operation condition setting for plasticizing process.

No.	Operating Parameter	Set Point
1	Nitrification degree of nitrocellulose (NC)	207 mL/g
2	The addition amount of NC	200 kg
3	The addition amount of diphenylamine (DPA)	2~4 kg
4	stirring time of DPA/ether mixed solvent	30 min
5	Jacket temperature of solvent preparation tank	22 °C
6	solvent/NC ratio	(18~25 °C)
7	Ether-ethanol solvent ratio	0.65~0.75:1
8	Stirring speed	1.0~1.2:1
9	Jacket temperature of the plasticizing machine	30 rpm
10	Forward stirring time	22 °C
11	Backward stirring time	(18~25 °C)
12	Interval time between forward and backward	240 s
13	Plasticizing time setting	60 s

The list of faults of this paper are shown in Table 3. The batch data of the plasticizing process under five typical fault conditions (the first three faults were caused by fluctuation of the single process variables, and the fourth and fifth were the abnormal operation conditions caused by the disturbance of raw materials and the under-voltage work of the stirring motor) were generated, which were used to verify the fault detection algorithm based on NMI-WMPCA, and were compared with the traditional MPCA and MPCA methods. The value of the confidence coefficient  $\alpha$  was set to 99%, and the principal component number *A* of each MPCA model was determined according to the cumulative variance contribution rate  $\geq 90\%$ . As the traditional MPCA and MI-MPCA methods require

the same batch data length, all 10 batches' lengths were set to 60 min during modelling. Obviously, MPCA and MI-MPCA will not be able to monitor the process when the operation time is longer than 60 min.

**Table 2.** Process variables for the modelling of the plasticizing process.

No.	Variable Description	Units
$x_1$	The addition amount of ether-ethanol mixed solvent and DPA	kg
$x_2$	Stirring speed of Agitator motor	rpm
$x_3$	Jacket cooling water valve opening	%
$x_4$	Jacket cooling water temperature	°C
$x_5$	Agitator motor current	A
$x_6$	Agitator shaft temperature T1	°C
$x_7$	Agitator shaft temperature T2	°C
$x_8$	Agitator shaft temperature T3	°C
$x_9$	Agitator shaft temperature T4	°C
$x_{10}$	Total plasticizing time	min

**Table 3.** List of faults introduced in the plasticizing process.

Case No.	Fault Description	Time (min)
F1	Step fault in stirring rate ( $x_2$ ) with magnitude increased by 5%	30–end
F2	Gradual fault in stirring speed ( $x_2$ ) with a speed of 0.1 rpm/min	30–end
F3	Gradual fault in jacket temperature ( $x_4$ ) with a speed of 0.1 °C/min	30–end
F4	Mismatch of raw material, artificial setting solvent/NC ratio of 0.55:1	0–end
F5	Abnormal operation of stirring motor, under-voltage operation with magnitude decreased by 10%	0–20

### 5.1. Fault Detection Results and Analysis of the Process Variable

The DCS control system of single-based gun propellant was developed using the PCS7 V9.0 system platform, and we used this platform to add the step and ramp signals to the key variables in the process as perturbations, in order to simulate and generate the first three fault conditions in Table 3. F1 is the faulty batch, where the stirring rate ( $x_2$ ) adds a step type fault from 30 min until the end of the process with an amplitude of 5%, and F2 is the faulty batch, where the stirring rate ( $x_2$ ) adds a ramp type fault from 30 min until the end of the process with change rate of 0.1rpm/min. Faulty batch F3 is a ramp type fault with a speed of 0.1 °C/min at a jacket cooling water temperature ( $x_4$ ) from 30 min until the end of the process.

Due to the limited length of the article, only the status monitoring chart of fault batch F2 is shown in this section. The monitoring results of the other fault batches can be found in Tables 4–6. Table 4 shows the comparison of the false alarm rates of fault batches F1, F2, and F3 by the three methods. Tables 5 and 6 are the statistical comparison of the fault detection time (FDT) and miss detection rate (MDR) of the five faulty batches by the three methods, respectively. It can be seen that, for step fault F1, although the amplitude of the stirring rate ( $x_2$ ) only fluctuates by 5%, the three methods can detect the fault quickly, which reflects the superiority of the data-driven multivariate statistical fault detection method. For ramp faults F2 and F3, the FDT of the three methods lags behind the fault occurrence time. This is because the fault variables change slowly at the beginning. When the fault variables gradually accumulate and deviate from the normal trend of change, the system can detect the abnormal changes in the process. At the same time, the monitoring performance of  $T^2$  statistics and  $SPE$  statistics is different, because  $T^2$  is a measure of the internal changes of the model, which reflects the deviation degree of each principal component in the amplitude and trend.  $SPE$  is a measure of the external changes of the model, which describes the deviation between the input variables and the

principal component model. In practical application, any statistics exceeding the limit can be considered as a fault.

**Table 4.** Fault detection error rate (FDER) based on different methods for the first three fault batches.

Fault No.	FDER (%)					
	MPCA		MI-MPCA		NMI-WMPCA	
	$T^2$	$SPE$	$T^2$	$SPE$	$T^2$	$SPE$
F1	2.7	4.4	1.7	2.2	0	0
F2	7.2	11.1	5	4.4	0	0
F3	7.7	10.5	5.5	5	0	0

**Table 5.** Fault detection time (FDT) based on different methods for all of the fault batches.

Fault No.	Fault Detection Time (FDT)					
	MPCA		MI-MPCA		NMI-WMPCA	
	$T^2$	$SPE$	$T^2$	$SPE$	$T^2$	$SPE$
F1	31.1	30.6	30.4	30.2	30.1	30.0
F2	56.3	47.1	39.3	37.1	34.4	34.2
F3	55.8	46.7	39.1	36.9	34.3	34.1
F4	55.3	29.6	40.7	21.9	14.8	5.2
F5	—	—	—	18.8	12.8	4.1

**Table 6.** Miss detection rate (MDR) based on different methods for all of the fault batches.

Fault No.	Miss Detection Rate (MDR)					
	MPCA		MI-MPCA		NMI-WMPCA	
	$T^2$	$SPE$	$T^2$	$SPE$	$T^2$	$SPE$
F1	3.9%	2.2%	1.6%	1.1%	0.5%	0.0%
F2	87.8%	57.2%	31.1%	23.9%	15%	13.9%
F3	86.1%	56.1%	30.5%	23.3%	14.4%	13.3%
F4	92.2%	49.4%	67.8%	36.4%	24.7%	8.6%
F5	100%	100%	100%	94.2%	64.2%	20.8%

Figures 4–6 show the monitoring results of fault batch F2 obtained by traditional MPCA, MI-MPCA, and the NMI-WMPCA algorithm in this paper, respectively. It can be seen that: (1) For the non-fault period (0–30 min), both the MPCA and MI-MPCA methods have high false positives. It can be clearly seen from the figure that many points exceed the control limit, and the fault detection error rate of the  $SPE$  statistics values reach 11.1% and 4.4%, respectively (see Table 4). This is mainly because MPCA and MI-MPCA need to estimate the future output values of the process through the current value, which make them too sensitive to the fluctuation data, and cause the false alarm rate to be increased. At the same time, the batch operation in the plasticizing process leads to a different initial state of the plasticizing machine before each batch of production, which is more likely to lead to false alarms in the early stage of plasticizing. However, NMI-WMPCA has avoided this problem well and effectively reduced the process false alarms. From Table 4, we can see that there was no false alarm for the first three faulty batches.

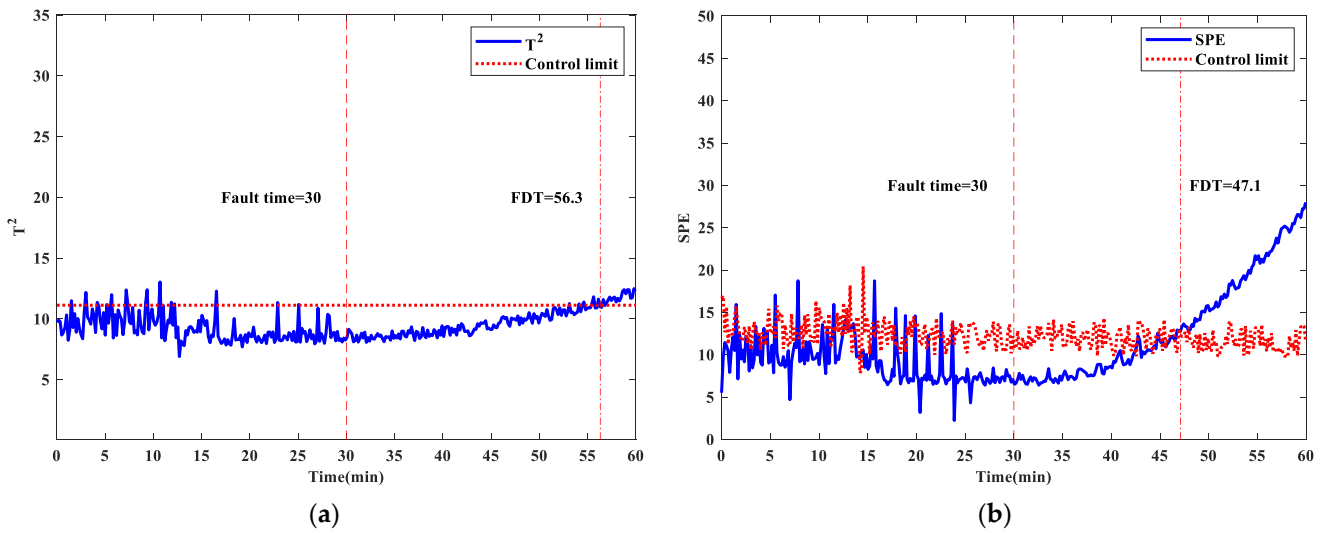


Figure 4. Fault monitoring charts of F2 based on MPCA: (a)  $T^2$  monitoring chart; (b) SPE monitoring chart.

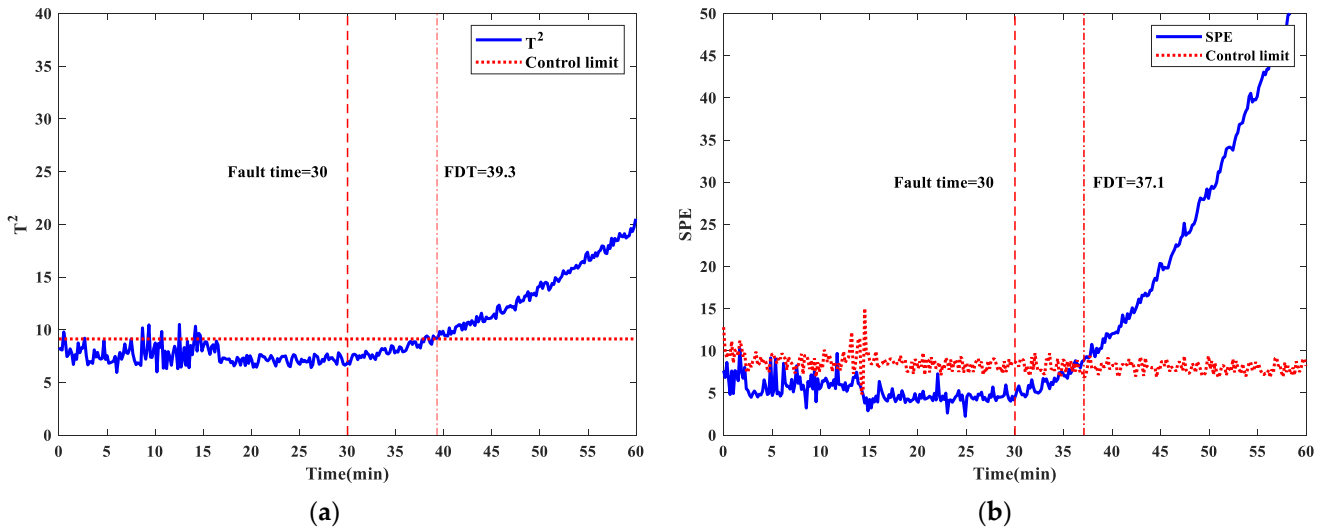


Figure 5. Fault monitoring charts of F2 based on MI-MPCA: (a)  $T^2$  monitoring chart; (b) SPE monitoring chart.

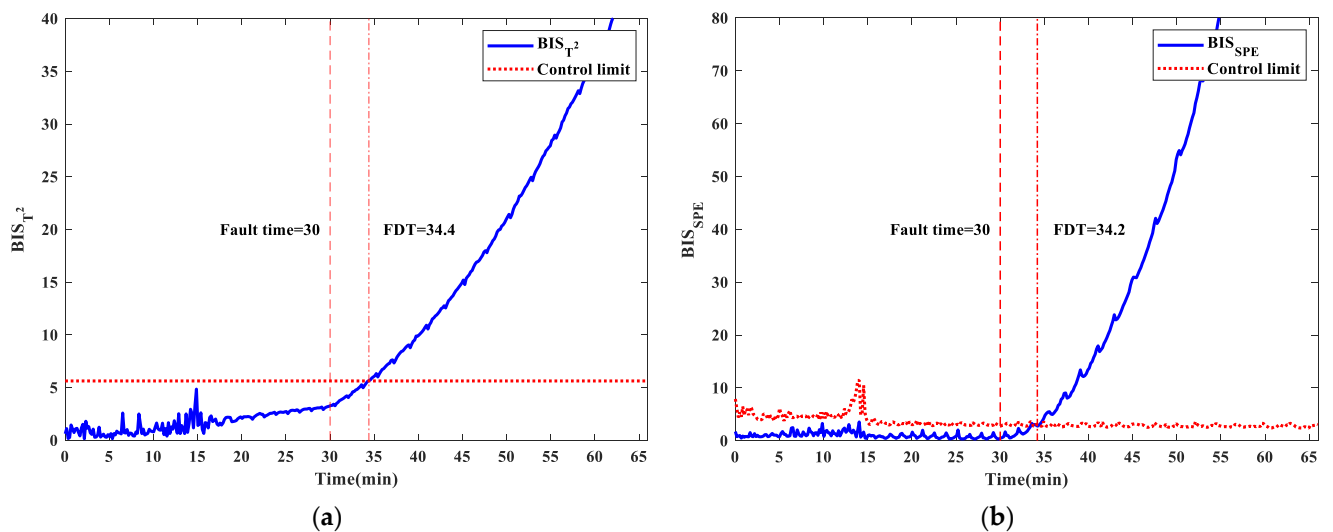


Figure 6. Fault monitoring charts of F2 based on NMI-WMPCA: (a)  $T^2$  monitoring chart; (b) SPE monitoring chart.

(2) For the fault period (after 30 min), the  $T^2$  and  $SPE$  statistics of the three methods all exceed the control limit at a certain time and continue to increase, indicating the occurrence of a gradual fault. By comparing the  $SPE$  statistics in Table 5, the  $BIS_{SPE}$  of NMI-WMPCA stably exceeds the limit at 34.2 min, in other words, NMI-WMPCA gives a fault warning only 4.2 min after the gradual fault was introduced, which is 12.9 min ahead of MPCA and 2.9 min ahead of MI-MPCA. For the NMI-WMPCA method, the fault detection ability of  $BIS_{T^2}$  statistics is slightly inferior to  $BIS_{SPE}$ , but greatly superior to the  $T^2$  statistics of the MPCA and MI-MPCA methods. The MDR in Table 6 also shows the superiority of NMI-WMPCA. The MDR of the  $SPE$  statistics is 13.9%, which is much higher than the 57.2% of the MPCA method and 23.9% of the MI-MPCA method. This indicates that the plasticizing process monitoring model established by the traditional MPCA and MI-MPCA methods cannot quickly identify the faults in the initial stage when the path of process variables deviates from the normal working condition.

(3) The actual running time of fault batch F2 is 66 min, with a total of 396 sampling points. For the time period beyond 60min, MPCA and MI-MPCA cannot realize the process monitoring, while NMI-WMPCA solves this problem through a two-stage unfolding method during modelling, so the model can alarm in time if the fault occurs in the period beyond 60 min.

According to the analysis above, the monitoring performance of the NMI-WMPCA method in this paper is better than that of the traditional MPCA and MI-MPCA methods. For the common small amplitude gradual faults in production, the traditional strategy of the rate of change over the limit can do nothing, so it can only be monitored by setting the alarm threshold. At present, the alarm threshold of the stirring speed ( $x_2$ ) and jacket cooling water temperature ( $x_4$ ) set on the DCS system are 33 rpm and 25 °C, respectively, and the alarm can only be made after 60 min. The NMI-WMPCA method proposed in this paper can realize early fault warning only about 4min after the fault occurs, detect the fault 26 min in advance, and facilitate operators to make decisions to adjust production in time, so that the process can return to the normal state.

## 5.2. Monitoring Results and Analysis of the Abnormal Operating Conditions

In order to verify the abnormal monitoring and evaluation ability of the method proposed in this paper, two failure conditions of raw material ratio imbalance and abnormal operation of the mixing motor were designed for testing. The former will affect the plasticizing effect and cause quality fluctuations. The latter will cause huge hidden dangers in production and endanger the safety of life and property.

### 5.2.1. Monitoring Results and Analysis of Raw Material Mismatch

During the plasticization process, the content of the ether-ethanol mixed solvent in the single-base gun propellant material will affect its rheological properties. When the solvent content is moderate, the plasticized chemicals have a uniform and compact structure with a smooth surface, without any defects such as hard materials and white spots. If the solvent/NC ratio is out of balance, it will cause the fluctuation of the plasticizing quality effect. A low solvent content will easily lead to poor fluidity of the materials, excessive moulding pressure, white spots, and other unqualified phenomena. It can also make the production process more dangerous. If the solvent content is too high, NC will be over-dissolved, and it will not be able to meet the requirements of a uniform and dense structure in the moulding process. In order to ensure the effect of the plasticizing quality, the solvent/NC ratio generally needs to be maintained between 0.65 and 0.75:1. The faulty batch F4 starts the plasticizing operation under the condition that the solvent/NC ratio is set to 0.55:1 to simulate the mismatch of raw material. The operation time of the batch is 64 min.

From the knowledge of the process mechanism, when the shear rate is constant and the solvent content increases, the apparent viscosity of the single-base gun propellant materials will decrease accordingly. Conversely, the decrease in solvent content increases the

apparent viscosity, which causes more shear heat to be generated during the plasticization process, which leads to the deviation of the coupling relationship between the trajectory of the process variables and the multi-dimensional variables from the normal operating conditions. From the monitoring results of the faulty batch F2, it can be seen that the monitoring performance of *SPE* is better than the  $T^2$  statistics. Therefore, only the *SPE* monitoring diagrams of each method are given below. The  $T^2$  statistics monitoring results can be seen in Tables 5 and 6. Figures 7–9 are the *SPE* monitoring results of the faulty batch F4 by the three methods, respectively. It can be seen from Figure 9 that the monitoring results of the NMI-WMPCA algorithm run smoothly, and can quickly identify abnormal operating conditions of the process. It stably exceeds the limit after only 5.2 min of process operation, and gives an early warning of failure. Combining Table 5 and Figures 7 and 8, it is 24.4 min ahead of MPCA and 16.7 min ahead of MI-MPCA. Thus the technologist can detect an abnormality of the plasticized materials in the current batch and take remedial measures in time, so as to avoid affecting the quality of the final product of the single-base gun propellant.

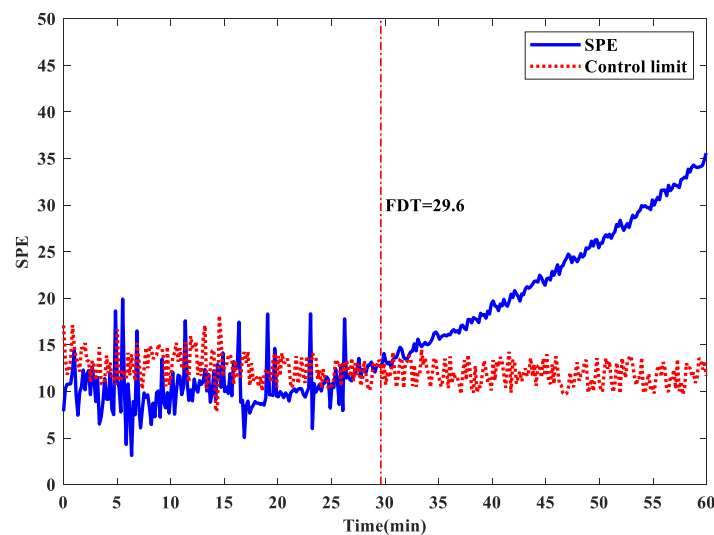


Figure 7. *SPE* fault monitoring chart of F4 based on MPCA.

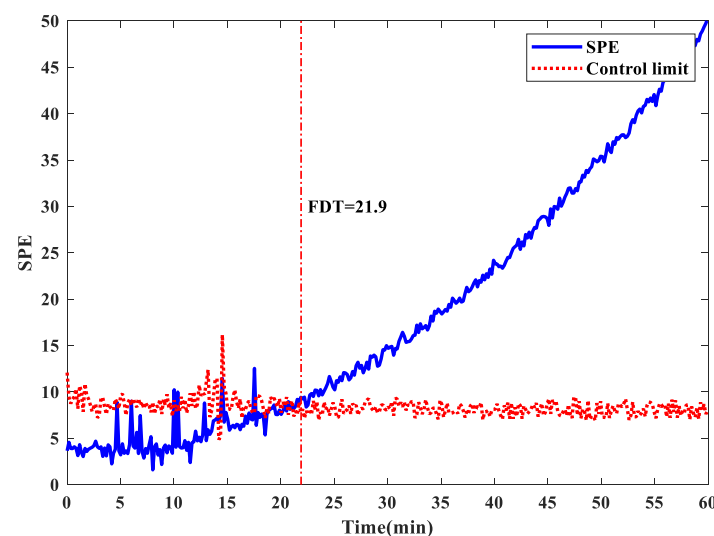


Figure 8. *SPE* fault monitoring chart of F4 based on MI-MPCA.

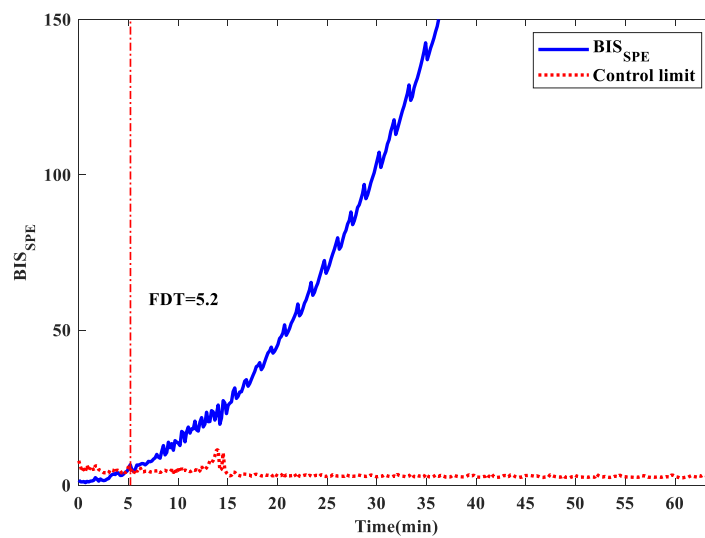


Figure 9. SPE fault monitoring chart of F4 based on NMI-WMPCA.

### 5.2.2. Monitoring Results and Analysis of Abnormal Operation of the Stirring Motor

In order to simulate the abnormal operation condition of the plasticizing process caused by the abnormal working condition of the stirring shaft, the faulty batch F5 reduces the working voltage of the stirring motor and makes it operate under the condition of under-voltage. It is known from the process mechanism that failure to reach the rated voltage will cause the motor speed to drop and the current to increase, and will cause the motor temperature to rise, which can burn the motor and cause a fire in severe cases.

Due to the potential safety hazard in the production of this fault, the under-voltage amplitude was set to 10% to ensure the safety of the process during the test, and the running time only lasted for 20 min. Because of the short running time of the faulty batch, the  $T^2$  and SPE statistics of the traditional MPCA did not form an effective monitoring for it. So, Table 5 only shows the monitoring results of the faulty batch F5 by MI-MPCA and the algorithm in this paper. Among them, as shown in Figure 10, the SPE statistics of MI-MPCA detect the fault just before the end of operation (18.8 min). The monitoring results of NMI-WMPCA are shown in Figure 11. The  $BIS_{SPE}$  statistic detects the abnormal working condition after 4.1 min of operation, and the fault warning is given in advance. This will force maintenance personnel to conduct troubleshooting, so as to effectively avoid the occurrence of safety accidents.

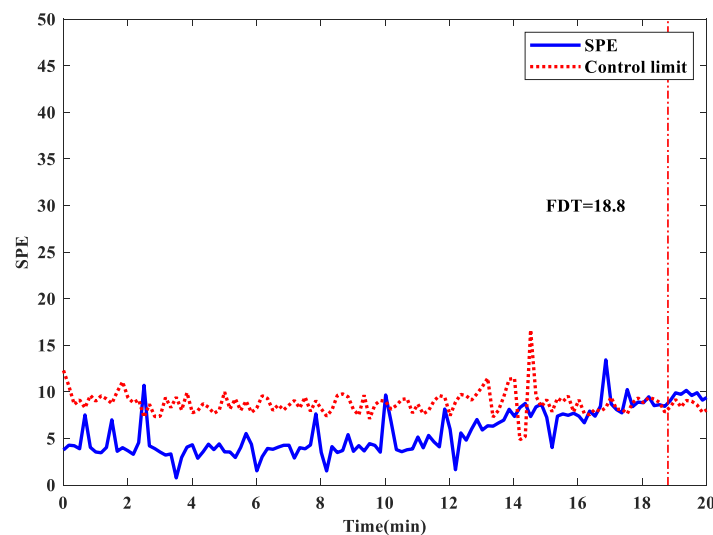
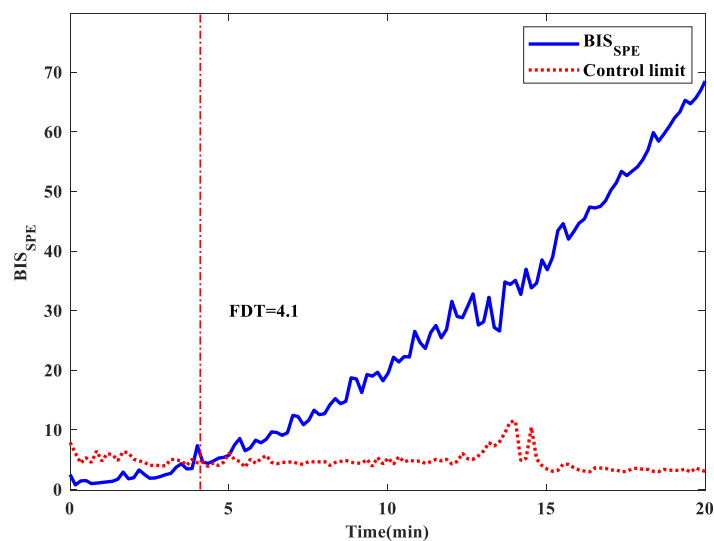


Figure 10. SPE fault monitoring chart of F5 based on MI-MPCA.



**Figure 11.** SPE fault monitoring chart of F5 based on NMI-WMPCA.

Careful observation of the monitoring performance results in Tables 5 and 6 also show that, with respect to the fault monitoring of the process variables, the gap between other methods and the NMI-WMPCA algorithm for abnormal operating conditions monitoring performance is further widened. An analysis of the reason for this may be because the abnormal operating conditions will change the coupling relationship between multiple variables in the process. MPCA can only handle the linear relationship among them. Although MI-MPCA can handle the mixed features of linear and non-linear correlation to a certain extent, the difference in correlation is not considered when modelling, and it cannot be compared with limited batch data. Class faults realize fast and effective monitoring and early warning. NMI-WMPCA uses normalized mutual information weighted correction to obtain a data set that fully reflects the coupling relationship between each variable and the other dimensional variables, and uses the generalization ability of multiple models to fully explore it under limited batch data containing a variety of correlation and mixing characteristics and correlation differences, to establish a coupling relationship model between multi-dimensional variables and realize the monitoring and early warning of abnormal working conditions.

### 5.3. Comparison and Analysis of Monitoring Results between Limited and Sufficient Batch Samples

The fault detection algorithm based on NMI-WMPCA is validated under five typical fault conditions with limited batch samples modelling, and is compared with the traditional MPCA and MI-MPCA methods. However, it is not compared with sufficient sample conditions. Therefore, a performance comparison experiment of three methods under limited batch samples modelling and sufficient batch samples modelling is added in this study. The ratio of the number of batch samples to the number of process variables under limited batch samples modelling is 1:1, while the ratio of the number of batch samples to the process variables under sufficient batch sample modelling is 4:1. That is, 40 batches of data are used as the training data sets. The experiment results are shown in the Table 7, and the data listed in the table are the monitoring results of the SPE statistics.

It can be seen from Table 7 that when the size of batch samples is sufficient, the detection performance of MPCA and MI-MPCA is greatly improved, especially for the detection performance of abnormal operating conditions. Taking the MDR index of faulty batch F4 as an example, the MPCA method increases by about 31% and MI-MPCA increases by 26.1%. This shows that when the size of batch samples is sufficient or relatively sufficient, MPCA and MI-MPCA can also establish a relatively stable monitoring model and can achieve good monitoring results. However, the two methods still have a high false alarm rate. By contrast, the detection performance of NMI-WMPCA is improved to some extent, but the improvement is not significant. The MDR of the faulty batch F4 increases by only

1.7%. It indicates that the outstanding advantage of mining the differences of the coupling correlation among multi-dimensional process variables and the mixed characteristics of multiple linear and nonlinear relationships lies in the good ability of fewer samples for modelling. The proposed method can establish an accurate and reliable fault detection model under limited batch sample modelling, and realize the rapid detection of multiple faults and the early warning of abnormal operating conditions. Furthermore, it has a good effect on eliminating false alarms in the process. When the sample size is sufficient, the monitoring performance is not greatly improved. However, when the batch samples are sufficient, the improvement of the monitoring performance is not very great.

**Table 7.** Performance comparison experiment results of three methods under limited batch samples modelling and sufficient batch samples modelling.

Algorithm	Size of Batch Samples	Performance Index (SPE)	Fault No.				
			F1	F2	F3	F4	F5
MPCA	Limited batch samples modelling	FDER	4.4%	11.1%	10.5%	—	—
		MDR	2.2%	57.2%	56.1%	49.4%	100%
		FDT	30.6	47.1	46.7	29.6	—
	Sufficient batch samples modelling	FDER	3.9%	9.4%	10%	—	—
		MDR	1.1%	32.8%	31.7%	18.1%	51.7%
		FDT	30.2	39.8	39.5	10.8	10.3
MI-MPCA	Limited batch samples modelling	FDER	2.2%	4.4%	5%	—	—
		MDR	1.1%	23.9%	23.3%	36.4%	94.2%
		FDT	30.2	37.1	36.9	21.9	18.8
	Sufficient batch samples modelling	FDER	1.7%	2.2%	2.7%	—	—
		MDR	0.6%	18.3%	17.2%	10.3%	29.2%
		FDT	30.1	35.5	35.2	6.2	5.8
NMI-WMPCA	Limited batch samples modelling	FDER	0%	0%	0%	—	—
		MDR	0%	13.9%	13.3%	8.6%	20.8%
		FDT	30.0	34.2	34.1	5.2	4.1
	Sufficient batch samples modelling	FDER	0%	0%	0%	—	—
		MDR	0%	10.6%	10.6%	6.9%	17.5%
		FDT	30.0	33.1	33.1	4.1	3.5

The advantages and disadvantages of the three methods are compared from 11 aspects. The results are shown in the Table 8. It can be seen clearly that NMI-WMPCA method has advantages in most aspects, but there are also inevitable problems such as more computation and complex modelling. However, these works are performed in the off-line modelling phase of the NMI-WMPCA method and have no effect on online fault detection.

**Table 8.** Comparisons of advantages and disadvantages of MPCA, MI-MPCA, and NMI-WMPCA.

Items Comparison	MPCA	MI-MPCA	NMI-WMPCA
Complexity of the model	Simple	Medium	Complex
Modeling efficiency	Fast	Medium	Slow
Fault detection error rate	High	Medium	Low
Miss detection rate	High	Medium	Low
Processing the uneven-length data of batches	No	No	Yes
Considering the difference in coupling correlation of variables	No	No	Yes
the coupling characteristics of linear and nonlinear relationships	No	Yes	Excellent
Detection performance under limited batch samples modelling	Poor	Medium	Excellent
Detection performance for the fault of process variables	Medium	Good	Excellent
Detection performance for the abnormal operating conditions	Poor	Medium	Excellent
Detection performance under sufficient batch samples modelling	Medium	Good	Excellent

#### 5.4. Fault Diagnosis Results and Analysis Based on NMI-WMPCA

The fault diagnosis method based on the multi-model *SPE* statistical contribution plot proposed in this paper is used to identify the fault source variables of the fault batches F2, F4, and F5 in turn. The *SPE* contribution graphs are shown in Figures 12–14, respectively. The red dashed line in the figure is the setting reference limit (10%). The variable index corresponds to the serial number in Table 2. When a fault is detected, priority is given to isolating the variables that exceed the reference limit. The fault batch F2 is that the stirring speed ( $x_2$ ) introduces a gradual fault with a change rate of 0.1 rpm/min in 30 min until the end of the process. It can be seen from Figure 12 that the contribution rate of the variable  $x_2$  is the highest, indicating that the proposed method can accurately diagnose the fault source variable. At the same time, the contribution rate of the stirring motor current feedback value ( $x_5$ ) also exceeds the reference limit. This is because the gradual change of the stirring rate will cause the fluctuation of the motor current. The method proposed in this paper can capture and characterize the correlation between them well.

The fault batch F4 is a fault that simulates the imbalance of the raw material ratio, which is an abnormal overall operating condition. It can also be seen from Figure 14 that many variables exceed the reference limit. Among them, the additional amount of ether-ethanol mixed solvent and DPA( $x_1$ ) contributes the most. At the same time, the decrease in solvent content causes more shear heat in the plasticizing process, which makes the opening of the jacket cooling water valve ( $x_3$ ) and the temperature of the stirring shaft ( $x_6\sim x_9$ ) deviate from the normal range. This information can be reflected in the contribution plot method proposed in this article. The direct cause of the faulty batch F5 is that the under-voltage work causes the motor speed to drop and the current to increase, and results in a rise of motor temperature. This makes the contribution rate of the stirring rate ( $x_2$ ) and the motor current ( $x_5$ ) in Figure 14 exceed the limit. Simultaneously, the stirring shaft temperature ( $x_6\sim x_9$ ) is also close to the reference limit. The fault diagnosis based on NMI-WMPCA can correct the model information according to the correlation difference between the variables, weaken the dimension of the variables with poor coupling correlation, and make the relationship of the variables with a strong correlation be reflected. The above results show that whether it is a process variable fault or an abnormal operating condition, the contribution plot method proposed in this paper can accurately identify the fault source variable, which can effectively assist maintenance personnel in troubleshooting and fault location.

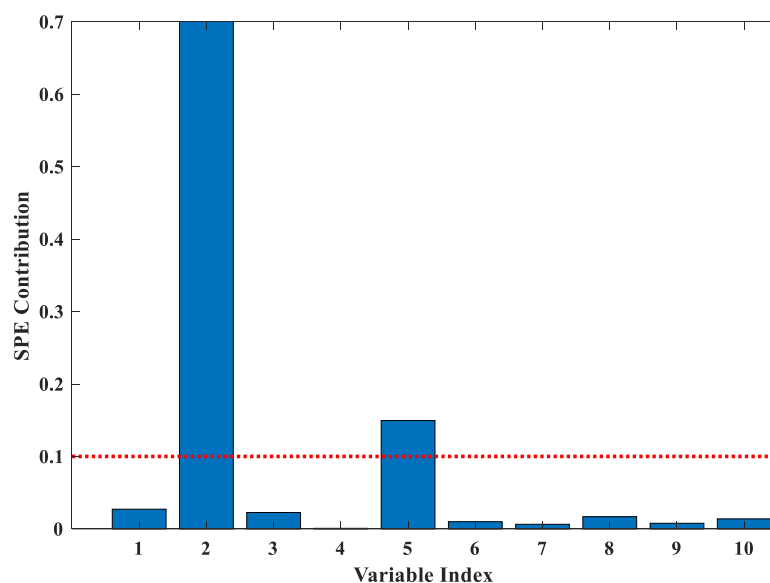


Figure 12. *SPE* contribution plot for fault diagnosis of F2 based on NMI-WMPCA.

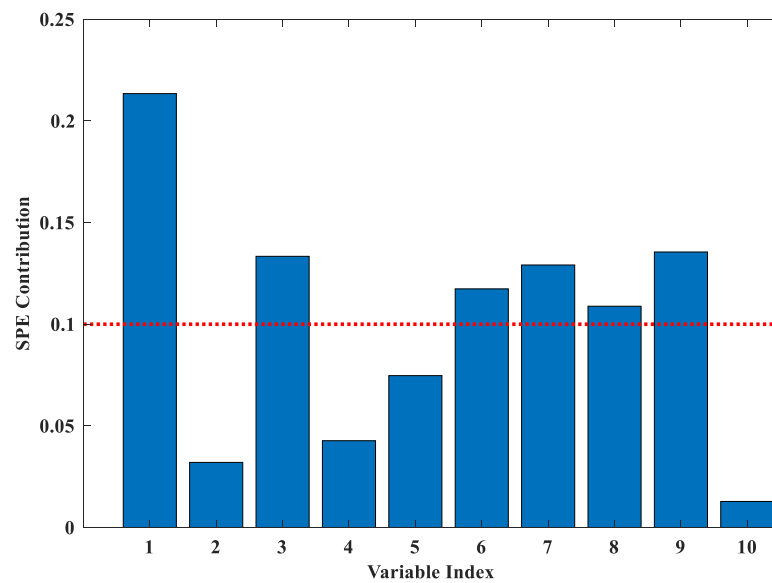


Figure 13. *SPE* contribution plot for fault diagnosis of F4 based on NMI-WMPCA.

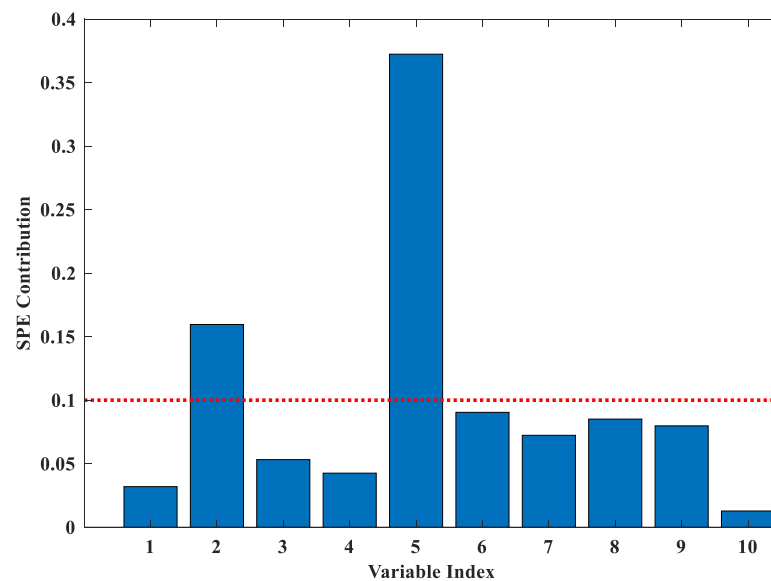


Figure 14. *SPE* contribution plot for fault diagnosis of F5 based on NMI-WMPCA.

## 6. Conclusions

The plasticizing process of single-base gun propellant lacks a reliable gradual fault detection ability and alarm evaluation under abnormal working conditions. Meanwhile, the differences in the coupling correlation among multi-dimensional process variables and the coupling characteristics of linear and nonlinear relationships in the process are considered. A fault detection and diagnosis method based on normalized mutual information weighted multiway principal component analysis (NMI-WMPCA) under limited batch sample modelling was proposed. In this method, the intricate coupling relationship between multidimensional variables is characterized by normalized mutual information, and the correlation between variables of different dimensions is modified by weight. NMI-WMPCA can utilize the generalization ability of the multi-model to establish an accurate fault detection model in limited batch samples, and adopts a fault diagnosis method based on a multi-model *SPE* statistic contribution plot to identify fault sources. The experimental results demonstrate that the proposed method is effective, which can realize the rapid detection and diagnosis of multiple faults in the plasticizing process by using only limited

batch sample modelling. It has a good sensitivity and the ability to capture early faults, and provides convenience for operators to take corresponding measures in time, to reduce the quality fluctuation and improve the safety of the process. Subsequently, how to achieve better monitoring results with a smaller sample size will be studied, as well as how to combine this with transfer learning to realize the fault detection and diagnosis of similar new processes.

**Author Contributions:** Conceptualization, M.Y. and J.W.; methodology, M.Y.; software, Y.Z. and X.B.; validation, M.Y. and X.X.; writing—review and editing, M.Y. and L.F.; supervision, Z.X.; project administration, M.Y. and Z.X. All authors have read and agreed to the published version of the manuscript.

**Funding:** This work was partially supported by the Youth Innovation Promotion Association CAS (2021203), the National Natural Science Foundation of China (61902299 and 61903357), the China Postdoctoral Science Foundation(2019TQ0239 and 2019M663636), the Liaoning Revitalization Talents Program (XLYC1902110), the Liaoning Provincial Natural Science Foundation of China (2019-YQ-09, 2020JH2/10500002, and 2020-MS-032), the Guangzhou Science and Technology Planning Project (202102021300), and the Scientific Research Project for Explosives and Propellants of China.

**Institutional Review Board Statement:** Not applicable.

**Informed Consent Statement:** Not applicable.

**Data Availability Statement:** The data presented in this study are available upon request from the first author. The data are not publicly available due to intellectual property protection.

**Conflicts of Interest:** The authors declare no conflict of interest.

## References

1. Jiang, Q.C.; Yan, X.F.; Huang, B. Review and Perspectives of Data-Driven Distributed Monitoring for Industrial Plant-Wide Processes. *Ind. Eng. Chem. Res.* **2019**, *58*, 12899–12912. [[CrossRef](#)]
2. Venkatasubramanian, V. The promise of artificial intelligence in chemical engineering: Is it here, finally? *AIChE J.* **2019**, *65*, 466–478. [[CrossRef](#)]
3. Gajjar, S.; Kulahci, M.; Palazoglu, A. Real-time fault detection and diagnosis using sparse principal component analysis. *J. Process Control* **2018**, *67*, 112–128. [[CrossRef](#)]
4. Reis, M.S.; Gins, G. Industrial Process Monitoring in the Big Data/Industry 4.0 Era: From Detection, to Diagnosis, to Prognosis. *Processes* **2017**, *5*, 35. [[CrossRef](#)]
5. Boulkadid, K.M.; Lefebvre, M.H.; Jeuniau, L.; Dejeaifve, A. Mechanical and Ballistic Properties of Spherical Single Base Gun Propellant. *Cent. Eur. J. Energetic Mater.* **2017**, *14*, 90–104. [[CrossRef](#)]
6. Yu, H.; Li, Z.; Liu, B.; Wei, L.; Zheng, S.; Han, B. Study on the Preparation and Properties of Modified Single-base Gun Propellant with High Nitrogen Content. *Chin. J. Explos. Propellants* **2018**, *41*, 632–636.
7. Trebinski, R.; Janiszewski, J.; Leciejewski, Z.; Surma, Z.; Kaminska, K. On Influence of Mechanical Properties of Gun Propellants on Their Ballistic Characteristics Determined in Closed Vessel Tests. *Materials* **2020**, *13*, 3243. [[CrossRef](#)]
8. Wang, Y.; Yang, H.; Han, J.; Gao, K. Effect of DGTN Content on Mechanical and Thermal Properties of Modified Single-based Gun Propellant Containing NQ and RDX. *Propellants Explos. Pyrotech.* **2020**, *45*, 128–135. [[CrossRef](#)]
9. Wang, Y.-Y.; Deng, G.-D.; Xu, J.; Wang, Z.-Q.; Gu, Q.; Zeng, J. A Rapid Determination Method of Deterrent Component Content in Single-base Gun Propellant. *Huozhayao Xuebao Chin. J. Explos. Propellants* **2018**, *41*, 408–413. [[CrossRef](#)]
10. Zhao, Q.-L.; Zhou, H.-W.; Chen, C.-L.; He, Y.; Zhang, W.-B.; Guo, L.-B.; Chen, G.; Yang, Q. Prediction Methodology of Function Failure Threshold Value of Deterred Gun Propellant for Firearms. *Huozhayao Xuebao Chin. J. Explos. Propellants* **2021**, *44*, 101–105. [[CrossRef](#)]
11. Zeman, S.; Jungova, M. Sensitivity and Performance of Energetic Materials. *Propellants Explos. Pyrotech.* **2016**, *41*, 426–451. [[CrossRef](#)]
12. Alauddin, M.; Khan, F.; Imtiaz, S.; Ahmed, S. A Bibliometric Review and Analysis of Data-Driven Fault Detection and Diagnosis Methods for Process Systems. *Ind. Eng. Chem. Res.* **2018**, *57*, 10719–10735. [[CrossRef](#)]
13. Apsimidis, A.; Psarakis, S.; Moguerza, J.M. A review of machine learning kernel methods in statistical process monitoring. *Comput. Ind. Eng.* **2020**, *142*, 12. [[CrossRef](#)]
14. Luwei, K.C.; Yunusa-Kaltungo, A.; Sha'aban, Y.A. Integrated Fault Detection Framework for Classifying Rotating Machine Faults Using Frequency Domain Data Fusion and Artificial Neural Networks. *Machines* **2018**, *6*, 59. [[CrossRef](#)]
15. Astolfi, D. Perspectives on SCADA Data Analysis Methods for Multivariate Wind Turbine Power Curve Modeling. *Machines* **2021**, *9*, 100. [[CrossRef](#)]

16. Gao, Z.; Liu, X. An Overview on Fault Diagnosis, Prognosis and Resilient Control for Wind Turbine Systems. *Processes* **2021**, *9*, 300. [[CrossRef](#)]
17. Gao, Z.; Chen, M.Z.Q.; Zhang, D. Special Issue on “Advances in Condition Monitoring, Optimization and Control for Complex Industrial Processes”. *Processes* **2021**, *9*, 664. [[CrossRef](#)]
18. Dong, Y.; Qin, S.J. A novel dynamic PCA algorithm for dynamic data modeling and process monitoring. *J. Process Control* **2018**, *67*, 1–11. [[CrossRef](#)]
19. Park, Y.J.; Fan, S.K.S.; Hsu, C.Y. A Review on Fault Detection and Process Diagnostics in Industrial Processes. *Processes* **2020**, *8*, 1123. [[CrossRef](#)]
20. Wang, R.; Edgar, T.F.; Baldea, M.; Nixon, M.; Wojsznis, W.; Dunia, R. A geometric method for batch data visualization, process monitoring and fault detection. *J. Process Control* **2018**, *67*, 197–205. [[CrossRef](#)]
21. Zhang, L.; E, D. Car dumper hydraulic system state monitoring and fault diagnosis based on adaptive MPCA. *Zhendong yu Chongji J. Vib. Shock* **2018**, *37*, 245–250, 256. [[CrossRef](#)]
22. Peres, F.A.P.; Peres, T.N.; Fogliatto, F.S.; Anzanello, M.J. Fault detection in batch processes through variable selection integrated to multiway principal component analysis. *J. Process Control* **2019**, *80*, 223–234. [[CrossRef](#)]
23. Zhou, J.; Huang, F.; Shen, W.; Liu, Z.; Corriou, J.-P.; Seferlis, P. Sub-period division strategies combined with multiway principle component analysis for fault diagnosis on sequence batch reactor of wastewater treatment process in paper mill. *Process. Saf. Environ. Prot.* **2021**, *146*, 9–19. [[CrossRef](#)]
24. Alcalá, C.F.; Qin, S.J. Analysis and generalization of fault diagnosis methods for process monitoring. *J. Process Control* **2011**, *21*, 322–330. [[CrossRef](#)]
25. Wang, Y.J.; Sun, F.M.; Jia, M.X. Online monitoring method for multiple operating batch processes based on local collection standardization and multi-model dynamic PCA. *Can. J. Chem. Eng.* **2016**, *94*, 1965–1976. [[CrossRef](#)]
26. Huang, J.P.; Yan, X.F. Relevant and independent multi-block approach for plant-wide process and quality-related monitoring based on KPCA and SVDD. *ISA Trans.* **2018**, *73*, 257–267. [[CrossRef](#)] [[PubMed](#)]
27. Zhang, S.M.; Wang, F.L.; Zhao, L.P.; Wang, S.; Chang, Y.Q. A Novel Strategy of the Data Characteristics Test for Selecting a Process Monitoring Method Automatically. *Ind. Eng. Chem. Res.* **2016**, *55*, 1642–1654. [[CrossRef](#)]
28. Yu, W.K.; Zhao, C.H. Robust Monitoring and Fault Isolation of Nonlinear Industrial Processes Using Denoising Autoencoder and Elastic Net. *IEEE Trans. Control Syst. Technol.* **2020**, *28*, 1083–1091. [[CrossRef](#)]
29. Pilario, K.E.; Shafiee, M.; Cao, Y.; Lao, L.; Yang, S.-H. A Review of Kernel Methods for Feature Extraction in Nonlinear Process Monitoring. *Processes* **2020**, *8*, 24. [[CrossRef](#)]
30. Tong, C.; Shi, X. Mutual information based PCA algorithm with application in process monitoring. *Huagong Xuebao CIESC J.* **2015**, *66*, 4101–4106. [[CrossRef](#)]
31. Jiang, Q.C.; Yan, X.F. Plant-wide process monitoring based on mutual information-multiblock principal component analysis. *ISA Trans.* **2014**, *53*, 1516–1527. [[CrossRef](#)]
32. Tong, C.; Lan, T.; Shi, X. Fault detection by decentralized dynamic PCA algorithm on mutual information. *Huagong Xuebao CIESC J.* **2016**, *67*, 4317–4323. [[CrossRef](#)]
33. Huang, J.P.; Yan, X.F. Quality Relevant and Independent Two Block Monitoring Based on Mutual Information and KPCA. *IEEE Trans. Ind. Electron.* **2017**, *64*, 6518–6527. [[CrossRef](#)]
34. Mori, L.; Yu, J. Maximized mutual information based non-gaussian subspace projection method for quality relevant process monitoring and fault detection. In Proceedings of the 52nd IEEE Conference on Decision and Control, Florence, Italy, 10–13 December 2013; pp. 4361–4366.
35. Aljunaid, M.; Tao, Y.; Shi, H. A Novel Mutual Information and Partial Least Squares Approach for Quality-Related and Quality-Unrelated Fault Detection. *Processes* **2021**, *9*, 166. [[CrossRef](#)]
36. Ge, Z.; Song, Z. Distributed PCA model for plant-wide process monitoring. *Ind. Eng. Chem. Res.* **2013**, *52*, 1947–1957. [[CrossRef](#)]
37. Tong, C.D.; Lan, T.; Shi, X.H. Fault detection and diagnosis of dynamic processes using weighted dynamic decentralized PCA approach. *Chemom Intell. Lab. Syst.* **2017**, *161*, 34–42. [[CrossRef](#)]
38. Jiang, Q.C.; Yan, X.F.; Huang, B.A. Performance-Driven Distributed PCA Process Monitoring Based on Fault-Relevant Variable Selection and Bayesian Inference. *IEEE Trans. Ind. Electron.* **2016**, *63*, 377–386. [[CrossRef](#)]
39. Zhao, C.H. Phase analysis and statistical modeling with limited batches for multimode and multiphase process monitoring. *J. Process Control* **2014**, *24*, 856–870. [[CrossRef](#)]
40. Pan, S.J.; Yang, Q. A Survey on Transfer Learning. *IEEE Trans. Knowl. Data Eng.* **2010**, *22*, 1345–1359. [[CrossRef](#)]
41. Wang, S.; Wang, D.; Kong, D.; Wang, J.; Li, W.; Zhou, S. Few-Shot Rolling Bearing Fault Diagnosis with Metric-Based Meta Learning. *Sensors* **2020**, *20*, 6437. [[CrossRef](#)] [[PubMed](#)]
42. Lu, J.Y.; Cao, Z.X.; Zhao, C.H.; Gao, F.R. 110th Anniversary: An Overview on Learning-Based Model Predictive Control for Batch Processes. *Ind. Eng. Chem. Res.* **2019**, *58*, 17164–17173. [[CrossRef](#)]
43. Shi, K.; Liu, Y.; Zhang, Z.; Yu, Q.; Zhang, Q. Constructing a Method for an Evaluation Index System Based on Graph Distance Classification and Principal Component Analysis. *Adv. Mater. Sci. Eng.* **2019**, *2019*, 6015754. [[CrossRef](#)]
44. Zhang, H.Y.; Tian, X.M.; Deng, X.G. Batch Process Monitoring Based on Multiway Global Preserving Kernel Slow Feature Analysis. *IEEE Access* **2017**, *5*, 2696–2710. [[CrossRef](#)]

45. Kammammettu, S.; Li, Z. Change point and fault detection using Kantorovich Distance. *J. Process Control* **2019**, *80*, 41–59. [[CrossRef](#)]
46. Qin, Y.; Zhao, C.H.; Wang, X.Z.; Gao, F.R. Subspace decomposition and critical phase selection based cumulative quality analysis for multiphase batch processes. *Chem. Eng. Sci.* **2017**, *166*, 130–143. [[CrossRef](#)]
47. Li, G.; Qin, S.J. Comparative study on monitoring schemes for non-Gaussian distributed processes. *J. Process Control* **2018**, *67*, 69–82. [[CrossRef](#)]
48. Wang, K.; Liu, J.; Wang, J.-Y. Learning Domain-Independent Deep Representations by Mutual Information Minimization. *Comput. Intell. Neurosci.* **2019**, *2019*, 9414539. [[CrossRef](#)] [[PubMed](#)]
49. Tang, Q.; Chai, Y.; Qu, J.; Fang, X. Industrial process monitoring based on Fisher discriminant global-local preserving projection. *J. Process Control* **2019**, *81*, 76–86. [[CrossRef](#)]
50. Gujrati, P.D. Jensen inequality and the second law. *Phys. Lett. A* **2020**, *384*, 6. [[CrossRef](#)]
51. Velázquez, J.C.; Caleyó, F.; Cabrera-Sierra, R.; Teran, G.; Hernandez-Sanchez, E.; Capula-Colindres, S.; Herrera-Hernández, H.; Ortiz-Herrera, C.C. A Bayesian Approach for Estimating the Thinning Corrosion Rate of Steel Heat Exchanger in Hydrodesulfurization Plants. *Adv. Mater. Sci. Eng.* **2018**, *2018*, 4314139. [[CrossRef](#)]